energies

MDPI

Article

Biomass and Coal Ash Sintering—Thermodynamic Equilibrium Modeling versus Pressure Drop Test and Mechanical Test

Karol Król, Wojciech Moroń and Dorota Nowak-Woźny *

Department of Energy Conversion Engineering, Faculty of Mechanical and Power Engineering, Wroclaw University of Science and Technology, 27 Wybrzeże Wyspiańskiego Street, 50-370 Wroclaw, Poland
* Correspondence: dorota.nowak-wozny@pwr.edu.pl

Abstract: The problem of biomass combustion and co-combustion is a particularly important aspect of many district heating systems, where the use of biomass makes it possible to reduce CO_2 emissions. The present article is a continuation of previous studies of the behavior of the mineral matter of selected fuels during the sintering processes. Three biomasses were studied: wheat straw, barley straw and rye straw, as well as two coals from Polish mines: bituminous coal and lignite. The study included ultimate and proximate analyses and oxide analysis. On the basis of the oxide analysis and using FactSage 8.0. software, the sintering process of ash from selected fuels was simulated. In particular, the content of the slag phase as well as the values of the specific heat c_p and density were determined without considering the gas phase. The obtained results were compared with the results of measurements of fracture stress (mechanical method) and pressure drop (pressure drop test) determined during the sintering process of the ash samples. The study showed that there is a fairly pronounced correlation between the sintering temperatures determined by the mechanical and pressure drop test and the physical properties of the ashes, such as density and heat capacity, and chemical properties, i.e., the content of the slag phase. The completed research work indicates and confirms that nonstandard methods of studying ash sintering temperatures (mechanical and pressure drop test) are very promising because they directly reflect the behavior of coals and biofuels in combustion systems.

Keywords: sintering; biomass; coal; FactSage; mechanical test; pressure drop test

Citation: Król, K.; Moroń, W.; Nowak-Woźny, D. Biomass and Coal Ash Sintering—Thermodynamic Equilibrium Modeling versus Pressure Drop Test and Mechanical Test. *Energies* **2023**, *16*, 362. https://doi.org/10.3390/en16010362

Academic Editor: Dimitrios Sidiras

Received: 25 November 2022
Revised: 20 December 2022
Accepted: 23 December 2022
Published: 28 December 2022

1. Introduction

The increasing energy demand and European regulations aimed at achieving carbon neutrality in 2040 [1] also place increasing demands on power units that use biomass as fuel in the combustion process. In particular, fuel with appropriate parameters is a matter of selecting fuel to ensure the greatest efficiency of the energy conversion process, which translates into lower carbon dioxide emissions per unit of final energy produced. When burning or cofiring biomass, the important fuel parameters that affect the final efficiency of the energy conversion process is the ash sintering temperature. This is particularly important in the case of biomass that contains a lot of alkali metals, particularly potassium and sodium, and also alkaline soils–calcium. The presence of these elements significantly affects the transformation of mineral matter, which, as a result, leads to a reduction in the melting temperature of the ash produced by the fuel combustion process [2–5]. At this temperature, sticky ash particles, which are the result of the combustion process, adhere to the boiler's heated surfaces during contact. Thus, over time, as a result of slagging and fouling processes, a hard layer is formed that impedes the heat transfer process inside the boiler and, thus, the efficiency of the energy conversion process is reduced. This leads to an increase in carbon dioxide emissions per unit of final energy. The additional cost, which translates into increased carbon dioxide emissions per unit of final energy, is due to the need to periodically remove the boiler from service to remove the layer of sintered ash [6].

Therefore, it is extremely important to correctly determine the ash sintering temperature of the fuel being burned.

The process of ash sintering, from a physical and chemical point of view, is very complex. This is due to the fact that the ash obtained from a given fuel is a collection of particles of matter that differ significantly from each other in their chemical composition, phase composition, crystal structure, and size and shape of individual grains [7,8]. In addition, the ash parameters mentioned in the previous sentence—that is, its microstructure—also depend on the fuel combustion temperature [9]. In addition, there are quite large differences between fuels and the same ash obtained from them. For example, the ash obtained from the combustion of a particular type of biomass may have a different microstructure depending on the soil in which the biomass was grown or on the climatic conditions found in a particular growing region [10].

In turn, the physical and chemical transformations of the microstructure of ash, especially biomass ash containing a relatively high amount of alkali oxides [11], directly affect the temperature of ash sintering. The key mechanism of the ash transformation process seems to be the melting of the surface of individual ash particles—particles become sticky. Such sticky grains start to coalesce due to the process of decreasing surface tension [12–14].

The ash deposits formed as a consequence of the coalescence of sticky ash particles (slagging in the radiative region and fouling in the convection region) cause an exploiting consequence, such as deterioration to the heat transfer, damage of boiler surfaces, and even the shutdown of the boiler [15]. It should also be mentioned that the build-up of the ash deposit is rather related to ash physicochemical properties of the ash, while its strength development depends more on ash sintering characteristics [16,17].

The formation of newly formed mineral phases and the transformation of the original minerals contained in the biomass can lead to difficulties in accurately determining the sintering temperature of the ash from a given fuel. There are many methods to evaluate the tendency, such as: oxide indices method, a purely empirical method based on many years of observations [18–21], the ash fusion test, based on visual observation of the change in the shape of the ash sample during the ash sintering process [2,22–25], or finally more physical methods directly based on observations of the change in the physical properties of ash samples, such as the failure stress—in the mechanical method [26], or the shrinkage of the sample and the change in its porosity—in the pressure method [26]. Other methods to be mentioned include: thermomechanical analysis [14], thermal conductivity analysis [27], electrical resistivity test [28], and other techniques presented in detail in [29]. Because the slagging and fouling process is associated with the formation of a molten ash phase [30], the thermochemical equilibrium calculation method is extremely important for research. This method allows us to predict the thermodynamically stable chemical and phase composition of sintered ash. In particular, the occurrence of thermodynamically stable melt phases is predicted based on thermochemical equilibrium calculations analysis. The application of the thermochemical equilibrium calculations method to predict the hazards of the slagging and fouling process has been experimentally supported in works [31–38], among others. Another interesting method for determining the hazards of the slagging and fouling process is also the electrical method, which has great potential for development, especially assuming AC measurements [39].

The article presented here complements the previously published results of studies [26] of the sintering temperature of biomass ash (and, for comparison, of coals as well) performed by non-standard methods: the mechanical test and pressure drop test. Research was supplemented with the results using FactSage 8.0 software. The vast majority of authors, when analyzing the results of research using FactSage software, focus only on the analysis of liquid phase formation. Therefore, in the work presented here, the goal was to verify the results of the strength and pressure tests of sintered ash with changes in density and specific heat of ash (predicted by FactSage) during the sintering process. The authors' goal was to demonstrate the suitability of the mechanical test and pressure drop test for the precise determination of the sintering temperature of ash from selected

fuels and to contribute to the understanding of the mechanism of the transformation of the mineral substance of fuels during their combustion. It was shown that there is a very good agreement between the results obtained using phase equilibrium thermodynamic analyses (FactSage 8.0) and the results of the strength–pressure method. The suitability of both methods for the precise determination of the sintering temperature was demonstrated.

2. Materials and Methods

In the work presented here, three biomasses were studied: rye straw (RS), barley straw (BS), and wheat straw (WS). Additionally, two coals from Polish mines were also selected as a reference: lignite (LC) from the Polish mine Bechatów and bituminous coal (BC) from the Polish mine Makoszowy. The ash from the selected fuels was produced according to European Standards [40]. For the study, ash with a grain fraction of 200 µm was selected (that is, fraction sizes with polydispersed dust consistencies that were in agreement with the generally applicable rules used for bituminous and lignite coals, according to the standard [41]). A detailed description of this process (ash production and its selection) can be found in [26], among others.

The technical analysis (in analytical state) was carried out according to Polish Standards for solid fuels [42–45]. The composition of the ashes was determined using the method of a Thermo iCAP 6500 Duo ICP plasma spectrometer using ASCRM-010 as a reference substance.

In the strength method, cylindrical specimens (8–8.5 mm in diameter and 10–12 mm in height) were first heated isothermally at 500 °C for 4 h and then quenched to room temperature. The samples prepared in this way were subjected to mechanical tests on the measuring system shown in Figure 1.

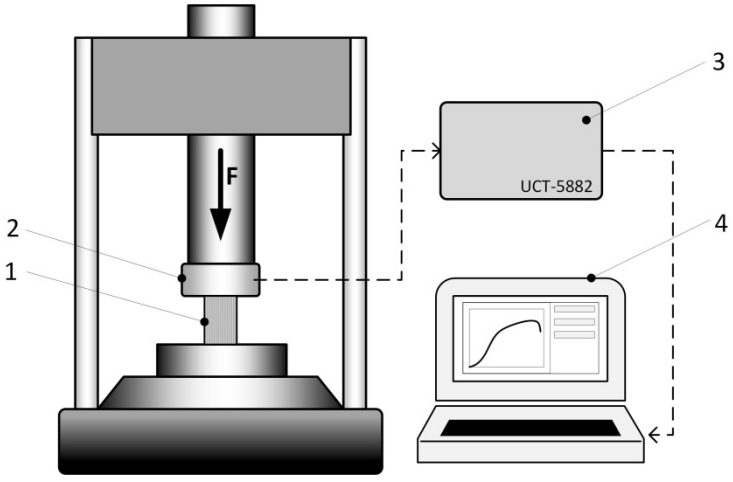

Figure 1. Mechanical test stand (1—sample, 2—hydraulic press, 3, 4—data acquisition and processing system).

This cycle was repeated for subsequent samples of the same ash quenched isothermally at a temperature 50 °C higher than that of the previous sample. These samples were quenched to room temperature and subjected to the same mechanical test. Measurements were repeated until the temperature reached about 1000 °C (depending on the fuel).

Sample preparation for the pressure drop test is the same as that described for the strength method. The only difference is how the sample is formed. For the pressure method, the sample (also in the form of a cylinder, but with a diameter of 10 mm and a height of 1.5 mm) is formed directly in the measuring tube (Figure 2). The exact method of measuring and forming the sample is described in [26].

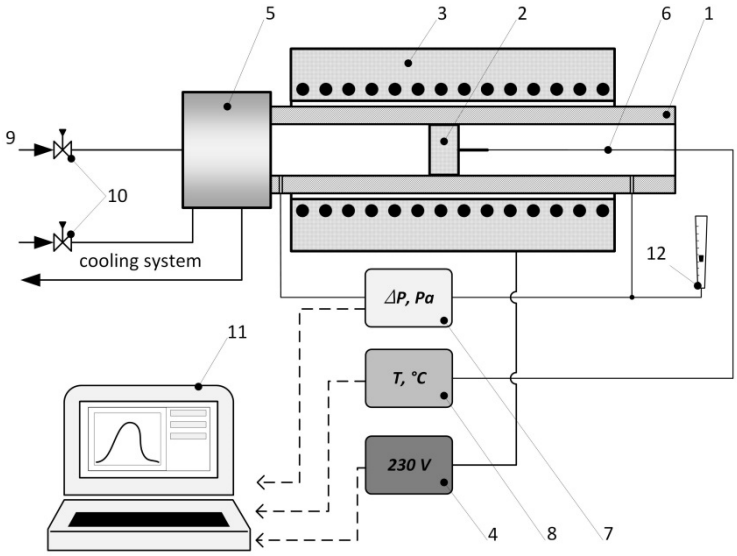

Figure 2. Pressure drop test stand (1—measuring tube, 2—sample, 3—furnace, 4—autotransformer, 5—radiator, 6—thermocouple, 7, 8—pressure gauge and thermometer, 9—compressed air, 10—fittings, 11—data acquisition and processing system, 12—rotameter).

Each mechanical and pressure measurement was repeated on five samples made from the same ash. The final results are the arithmetic mean and the uncertainty is the mean standard deviation.

FactSage 8 thermochemical software with databases was used to verify the mechanical test and the pressure drop test. FactSage is based on a combination of the Gibbs minimum free energy determination tool and thermodynamic equilibrium chemical simulation software. The assumption was made that there was one slag phase, and the FToxid, FTmisc, ELEM, and FactPS databases were used. The atmosphere was also excluded.

Details of the methodology and validity of the assumptions made can be found in the previous work [19]. The oxide content of the ashes was entered as input data. Thermodynamic calculations were carried out at temperatures from 500 to 1100 °C (in 20 °C increments) under a pressure of 0.1 MPa.

3. Results and Discussion

3.1. Samples Analsyis

The fuels selected for the study are characterized by a wide range of fuel properties. These include both coal and biomass currently used in the power and heating industries. Detailed proximate and final analysis data used in the article are provided in [26], while Figures 3 and 4 show only selected properties necessary for the presentation of the research results provided in this article.

Analyzing the data in Figure 3, it can be seen that the mineral content is the highest for LC (19.5 wt.%) while the lowest for WS and RS (3.7 wt.% and 3.6 wt.%, respectively). This would suggest that biomasses that have less mineral matter will perform more favorably in the combustion process, but the oxide composition of the ash of these biomasses (more extensively presented in [26]) highlights, increased CL, and increased basic to acidic oxides (B/A) ratio. The VM and the FC also show different properties of the biomasses, with almost twice the VM and almost twice the FR compared to the coals.

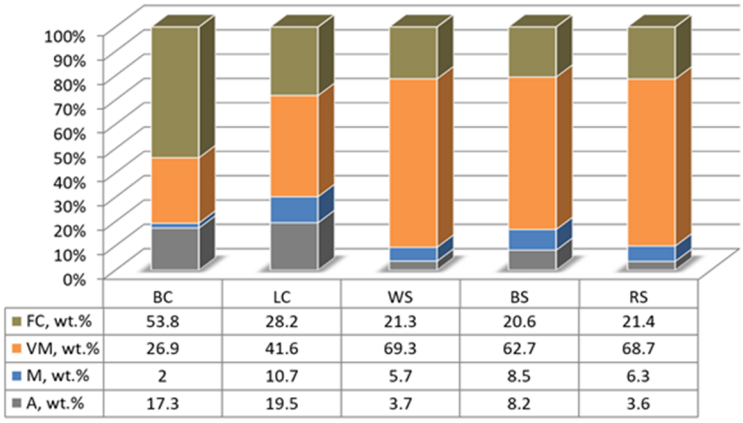

	BC	LC	WS	BS	RS
FC, wt.%	53.8	28.2	21.3	20.6	21.4
VM, wt.%	26.9	41.6	69.3	62.7	68.7
M, wt.%	2	10.7	5.7	8.5	6.3
A, wt.%	17.3	19.5	3.7	8.2	3.6

Figure 3. The proximate analysis (A—ash, M—moisture, VM—volatile matter, FC—fixed carbon) of fuel samples on air dried basis; BC—bituminous coal, LC—lignite, WS—wheat straw, BS—barley straw, RS—rye straw.

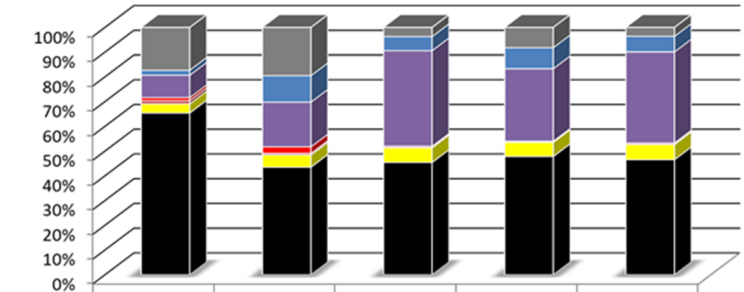

	BC	LC	WS	BS	RS
A, wt.%	17.3	19.5	3.7	8.2	3.6
M, wt.%	2	10.7	5.7	8.5	6.3
O, wt.%	9.1	18.1	38.6	29.3	36.8
S, wt.%	1.2	2.6	0.08	0.09	0.08
N, wt.%	1.3	0.7	0.6	0.4	0.6
H, wt.%	3.7	4.9	5.9	5.7	6.1
C, wt.%	65.4	43.5	45.4	47.8	46.5

Figure 4. Ultimate analysis (C, H, N, S, O and moisture (M) and ash (A) of the fuel samples on air dried basis; BC—bituminous coal, LC—lignite, WS—wheat straw, BS—barley straw, RS—rye straw.

These characteristic parameters of biomasses enforce the need for proper planning of the biomass combustion process. The biomass combustion process also differs from the coal combustion process in that the bulk of the energy in the case of coal combustion comes from the combustion of coke residue. Worthy of special attention also is the mineral content of these fuels. As shown in the article [26], biomasses have a high risk of adverse effects of a mineral substance on the combustion system, which on the one hand have very little mineral substance compared to coals, but the mineral substance contained therein is significantly more "aggressive" for the entire combustion system than the mineral substance of coal. This necessitates the need for proper organization of the combustion process, the use of protective coatings of heated surfaces, or other protective treatments.

By analyzing the data from the final analysis (Figure 4), it can be concluded that the fuels described in the article have very similar elemental composition. The elemental content of C varies from a maximum value for BC (65.4 wt.%) to a minimum value for LC (43.5 wt.%). On the other hand, the main difference between these fuels can be seen in the content of S and O. It can be noted that biomasses have no sulfur in their structure, while they have an increased proportion of oxygen compared to coals. The lack of sulfur in biomass simplifies the combustion system itself, but the increased share of oxygen forces a reorganization of the combustion process and shifts it from the area of burning coke residues (which is characteristic of coal fuels) to burning mainly volatile parts in

the case of biofuels. This behavior of the combustion process can promote an increase in the temperature of the flue gas along the height of the combustion chamber, which can adversely affect the retention of mineral matter, especially in the case of biomasses, which have lower ash sintering temperatures.

The consequence of higher temperatures in the upper zones of the combustion chamber can be an increased risk of slagging and fouling processes on the bulkhead heaters and the initial convection zones of the boiler. Therefore, the correct determination of the ash sintering temperatures becomes a particularly important issue. The study of [26] shows that the use of the classical Leitz test leads to the fact that the ash sintering temperatures determined on this basis are much higher than those occurring in reality. Therefore, nonstandard methods based on the study of changes in the physical and physicochemical properties of ash during its sintering are more reliable. Particularly noteworthy here are methods such as the pressure method and the strength method [26] based on measurements of the physical properties of ash.

The article presented here focuses in particular on comparing changes in physical quantities of ash as its specific heat and density (FactSage 8.0) with the results of the pressure drop test and mechanical test. The aim of continuing research is to develop a reliable, robust, and repeatable method for determining the sintering temperature of biomass ash. This is important both from the point of view of designing biomass combustion/co-firing boilers and from the point of view of the need to reduce CO_2 emissions.

Figure 5 shows the heating value (HHV) and fuel ratio (FR) for selected fuels. The FR value was calculated using the following formula: FR = FC/VM [26]. It can be seen that both biomass (WS, BS, and RS) and lignite (LC) have comparable HHV values. The exception is bituminous coal (BC), for which the HHV value is almost twice as high as for the other fuels (Figure 5a). Furthermore, the FR value for BC is about four times higher compared to the other selected fuels (Figure 5b). When analyzing the HHV and FR values of the selected fuels, we conclude that we can divide the selected fuels into three distinct groups. The first group includes RS, BS, and WS biomasses with relatively low HHV and FR values. The second group includes LC with HHV values comparable to those of biomass but with FR values higher than those of biomass but much lower than those of BC. In the last group, BC with high HHV and FR values. In this way, fuels belonging to three groups differentiated by technical parameters and sintering potential were selected.

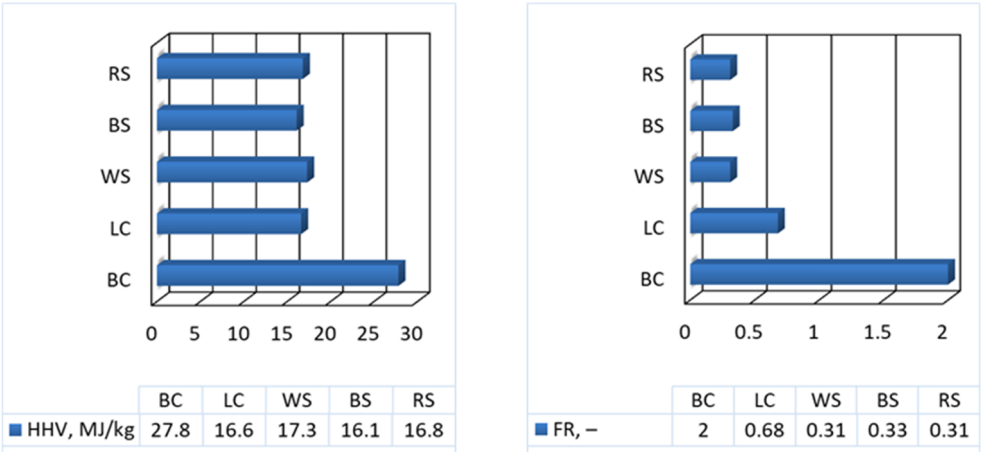

Figure 5. Characteristics of the tested fuels: (**a**) heating value (HHV) and (**b**) fuel ratio (FR).

The oxide composition of the ash from selected fuels (determined by the Thermo iCAP 6500 Duo ICP plasma spectrometer method using ASCRM-010), is shown in Figure 6.

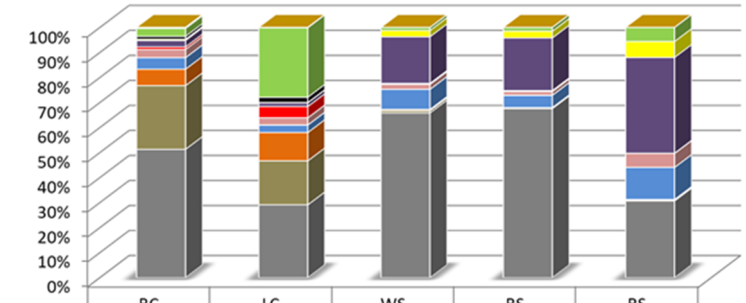

	BC	LC	WS	BS	RS
SrO	0.1	0	0	0	0
BaO	0.2	0	0	0	0
Mn3O4	0.1	0.1	0	0	0
SO3	3.2	27.8	1.2	1.5	5.6
TiO2	1.1	2.1	0	0	0
P2O5	0.5	0.1	2.5	2.7	6.4
K2O	2.6	1.5	18.6	21	38.3
Na2O	1	4.5	0.4	0.4	0.1
MgO	3.3	2.9	2	1.5	5.6
CaO	4.6	3	8	4.9	12.8
Fe2O3	6.6	11.3	0.5	0.2	0.3
Al2O3	25.5	17.6	0.9	0.2	0.3
SiO2	51.4	29.1	65.8	67.5	30.7

Figure 6. Composition from the ash of tested samples (wt.%).

The oxide composition of the ash is the basis for determining oxide indices, which are commonly used to characterize the tendencies of ash deposition. In a previous paper [26], the authors showed that the fuels studied have a high potential for the tendency to ash deposition due to the high content of silica, which reacts with sodium and potassium to form eutectics with low melting points. Furthermore, the chlorine content, which is responsible for the formation of potassium chloride and the formation of ash deposits on low-temperature heating surfaces, is very high for both coals, high for rye and barley straw and medium for wheat straw. On the contrary, the basic to acid ratio, which describes the general melting behavior, is low for all samples, except for rye straw, for which this ratio is high. There is a tendency to agglomerate the bed during fluidized bed combustion (BAI index)—for all tested biomass, it is below the limit and for both coals, it is above. The Babcock index (Rs), which provides some information about increasing the deposition tendency on high-temperature heating surfaces, is medium for lignite and low for other tested fuels. It suggests that tested biomass and bituminous coal are characterized by a low risk of ash deposition. Furthermore, the viscosity index is in the low value range for barley straw, wheat straw, and bituminous coal. However, for rye straw and lignite, it is in a high range.

In contrast, as previously presented in [26], the temperature of the initial deformation temperature (IDT) is the highest for bituminous coal (1030 °C) and the lowest for lignite (910 °C), wheat straw (790 °C), barley straw (760 °C) and rye straw (730 °C). These data, presented in detail in [26], show a certain conflict of index indications. Therefore, it is difficult to clearly determine the degree of risk associated with the slagging and fouling process based solely on the chemical composition of solid fuels.

3.2. FactSage Analysis versus Pressure Drop Test and Mechanical Test

For the ash samples tested, a comparison was carried out between the results obtained from thermodynamic equilibrium calculations of ash multicomponent systems and the results of sintering temperature measurements using a mechanical test and a pressure drop test. Figures 7–9 show a comparison of the pressure drop observed during the ash sintering process (measured on the bench shown in Figure 2) with the values of the ash density calculated at equilibrium, as well as with the values of the heat capacity c_p also calculated at equilibrium. The density and specific heat capacity values were determined

using FactSage 8.0 software. The density of the ash at equilibrium did not include the gas phase.

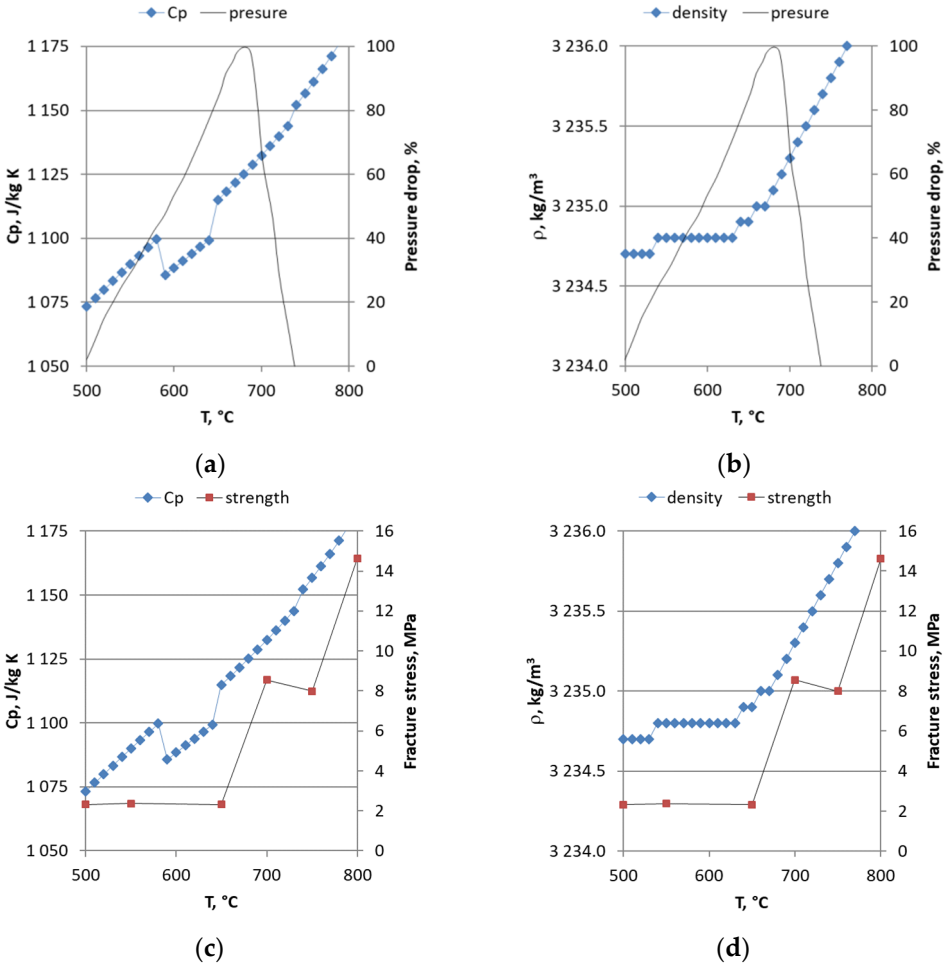

Figure 7. Rye straw: (**a**) Specific heat (c_p) and pressure drop as a function of temperature; (**b**) density (ρ) and pressure drop as a function of temperature; (**c**) specific heat and fracture stress as a function of temperature; (**d**) density and fracture stress as a function of temperature.

Analyzing the measured data of the pressure drop test realized during the ash sintering process obtained from rye, barley and wheat straw in comparison with the calculations obtained after using the FactSage 8.0 software, it was found that the temperature at which a clear pressure drop begins corresponds to a clear change in the nature of the density–temperature relationship. Interestingly, for rye straw, the sharp increase in density tends to be responsible for the shrinkage of the entire sample during sintering. The situation is slightly different for barley and wheat straw, for which a decrease in the density of ash is observed with a decrease in the pressure drop in the measuring system. It is believed that in the case of barley and wheat straw, we are unlikely to have a shrinkage of the entire ash sample during its sintering, but only a change in its microstructure that involves an increase in porosity and the formation of air transport channels through the sample.

Thus, we see that for the biomasses studied, we do not have a uniform process mechanism responsible for the pressure drop in the pressure method. However, it is interesting to note the close relationship between the pressure drop in the pressure method used to assess the sintering temperature measurement and the changes in solid ash density observed in Figures 7–9.

Analogous observations relate changes in ash density to the results of a mechanical test that involved the measurement of fracture stress. A sharp increase in fracture stress can

be associated with pronounced changes in density. The pronounced increase in fracture stress observed for rye straw biomass occurs at the same temperatures as the increase in density predicted using the FactSage 8.0 software. For this biomass, the increase in fracture stress values is related to chemical and physicochemical changes in the ash itself. For the other biomasses, on the other hand, good agreement can be found in terms of changes in both fracture stress and ash density, but the density decreases. The differences in the direction of density changes between the rye biomass and the other two biomasses are confirmed in Figure 10, which shows the formation of the liquid slag phase (calculation of the equilibrium of FactSage 8.0). The course of the dependence of slag (wt.%) versus T (°C) for RS biomass differs significantly from the course of the curves for the BS and WS biomasses (significantly lower values, especially in the initial phase at temperatures from 600 °C to 900 °C). This interesting observation supports the thesis regarding the very complex nature of the ash.

Of course, from the physicochemical side, the observed behavior of biomass ash is extremely interesting not only from the application side but also from the scientific side; nevertheless, it requires further research.

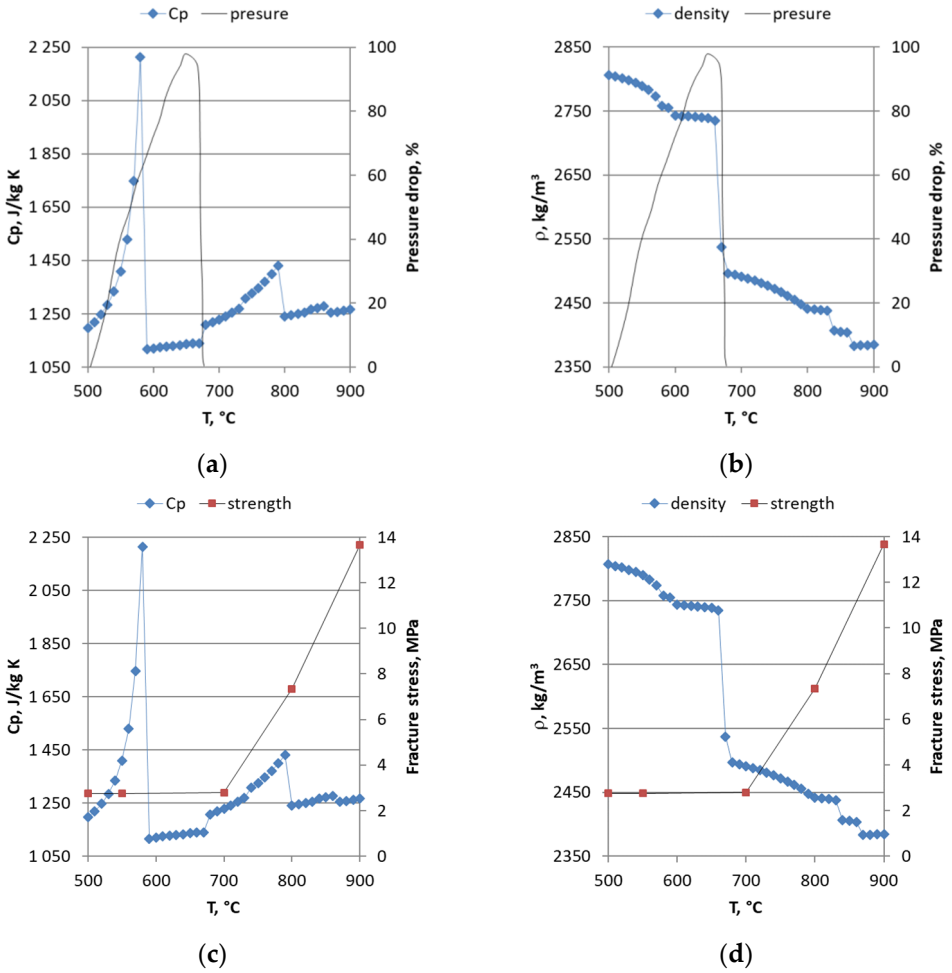

Figure 8. Barley straw: (**a**) Specific heat (c_p) and pressure drop as a function of temperature; (**b**) density (ρ) and pressure drop as a function of temperature; (**c**) specific heat and fracture stress as a function of temperature; (**d**) density and fracture stress as a function of temperature.

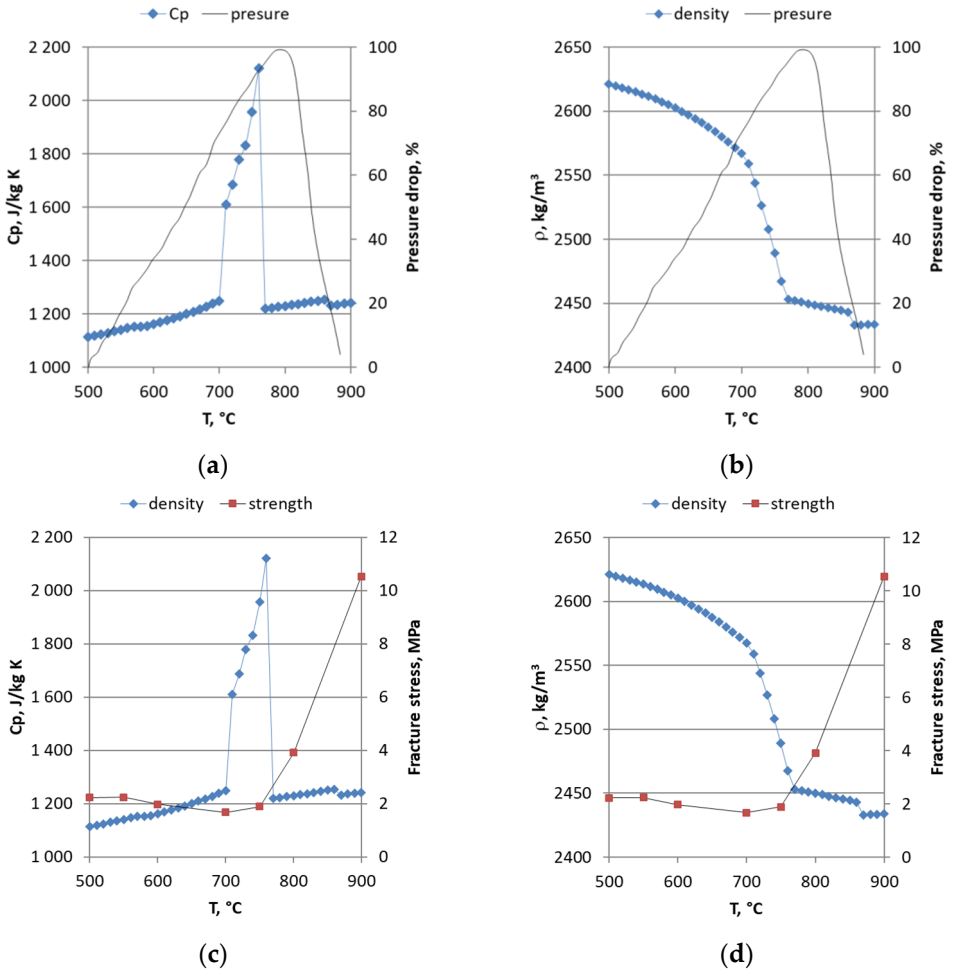

Figure 9. Wheat straw: (**a**) Specific heat (c_p) and pressure drop as a function of temperature; (**b**) density (ρ) and pressure drop as a function of temperature; (**c**) specific heat and fracture stress as a function of temperature; (**d**) density and fracture stress as a function of temperature.

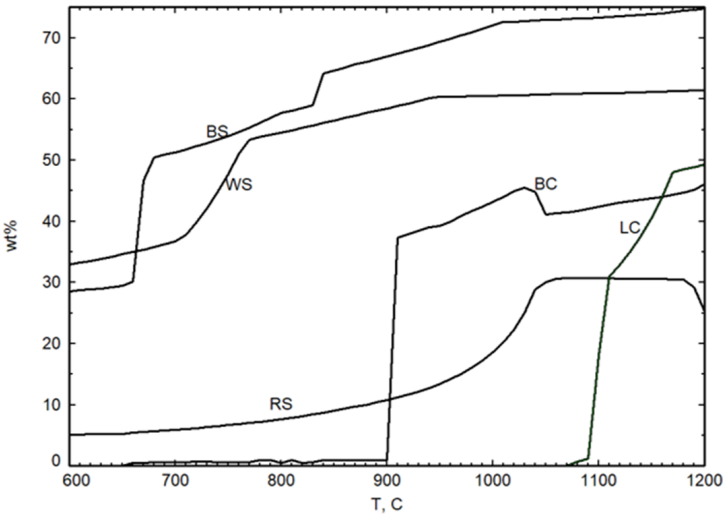

Figure 10. Phases of slag in equilibrium for rye straw (RS), wheat straw (WS), barley straw (BS), lignite (LC), and bituminous coal (BC).

For the biomasses studied, the specific heat of c_p for equilibrium was also calculated using FactSage 8.0 software. The results are shown in Figures 7–9. For rye straw biomass

(Figure 7a,c), the dependence of the specific heat of ash on the sintering temperature has three fairly distinct points of discontinuity. The first two points of discontinuity in c_p (for approximately 580 °C and 650 °C) coincide with the change in the slope of the pressure-drop–temperature-dependence in the range before the maximum is reached. Meanwhile, the third point for about 740 °C coincides with the complete unsealing of the sample in the measuring tube (pressure drop equal to zero). Analyzing the course of the dependence of c_p on temperature and comparing it with the course of the value of fracture stress on temperature (Figure 7c), it can be seen that the second and third points of discontinuity of c_p correspond to the increase in fracture stress.

For other biomasses, i.e., barley and wheat straw, the observed c_p discontinuities are even more pronounced. In the case of barley straw (Figure 8a,c), there are two distinct points of c_p discontinuity in the temperature range of changes in the pressure drop test, i.e., from 500 °C to 700 °C. The first discontinuity point, observed at around 600 °C, can be associated with a pronounced change in the slope of the pressure drop curve. The second discontinuity point occurring at about 680 °C falls, as in the case of rye straw, exactly at the point of complete unsealing of the sample in the measuring tube (pressure drop equal to zero). Analyzing Figure 8c, it can also be seen that the second discontinuity point c_p is associated with an increase in fracture stress. In addition, analyzing Figure 10, showing the slag phase content predicted by FactSage 8.0, it can be seen that the second c_p discontinuity point associated with complete unsealing of the sample in the test tube (pressure drop = 0 for 680 °C) can be associated with an increase in slag phase content from 29 wt.% to more than 50 wt.%.

For wheat straw, there are two very clear points of discontinuity and one rather subtle one. The first point of discontinuity c_p occurs at 700 °C and corresponds to a change in the slope of the pressure drop dependence on temperature. The second discontinuity point occurs at 780 °C and is located near the point of maximum pressure drop (Figure 9a). Additionally, the second point of discontinuity (for 780 °C) coincides with the point of increase in fracture stress (Figure 9c). When comparing the described data with the results of the slag phase (Figure 10), it is also possible to see the correlation of the c_p discontinuity points with changes in the content of the ash.

Interpretation of the correlation of specific heat c_p calculated for the equilibrium state of ash from the biomasses studied using the FactSage 8.0 software brings us a lot of new information about the mechanism of mineral transformations during sintering. However, it does not provide an unambiguous interpretation from a modeling point of view, allowing us to build a universal model of the mechanism of biomass ash transformations. This requires further research into the physiochemistry of biomass ash.

In particular, by analyzing the content of the slag phase and pressure drop profile, good agreement can be observed for the biomass of barley straw, wheat straw biomass and bituminous coal. On the contrary, for rye straw biomass and lignite coal, this effect is not observed. These discrepancies may be related to the alkali content and the composition of the oxidizing atmosphere during the combustion of wood fuels. In the thermodynamic studies presented here, the atmosphere was not taken into account. A recent study [46] shows that both the atmosphere and the alkali content can strongly affect the results of thermodynamic analysis. A thorough explanation of the observed discrepancies requires continued research.

For comparison, analogous tests were carried out for selected coals from Polish mines: lignite (LC) and bituminous coal (BC) (Figures 11 and 12). In the case of lignite, both density and c_p show more points of discontinuity than the analogous quantities for biomasses. This is understandable as a result of fuels with different natures such as biomasses and coals. Coal contains much more mineral matter, characterized by a certain crystalline structure, than biomass. Therefore, for coals, we observe many more density and c_p discontinuity points associated with phase transformations. Thus, for lignite, in the temperature range studied, we have as many as four discontinuity points for c_p and five for density. The same is true for bituminous coal (Figure 12). All the points of discontinuity for c_p and density

are related to the change in the slope of the pressure drop dependence on temperature, just as we found for biomasses. Additionally, as for biomasses, it is possible to observe an association of the point of discontinuity of both c_p and density with a change in fracture stress (Figure 11c,d and Figure 12c,d). Obviously, the temperature values for which a sharp drop in pressure and an increase in fracture stress are observed, that is, the appearance of ash sintering [26], are higher than for biomasses. This is related to the chemical composition of biomasses and coals.

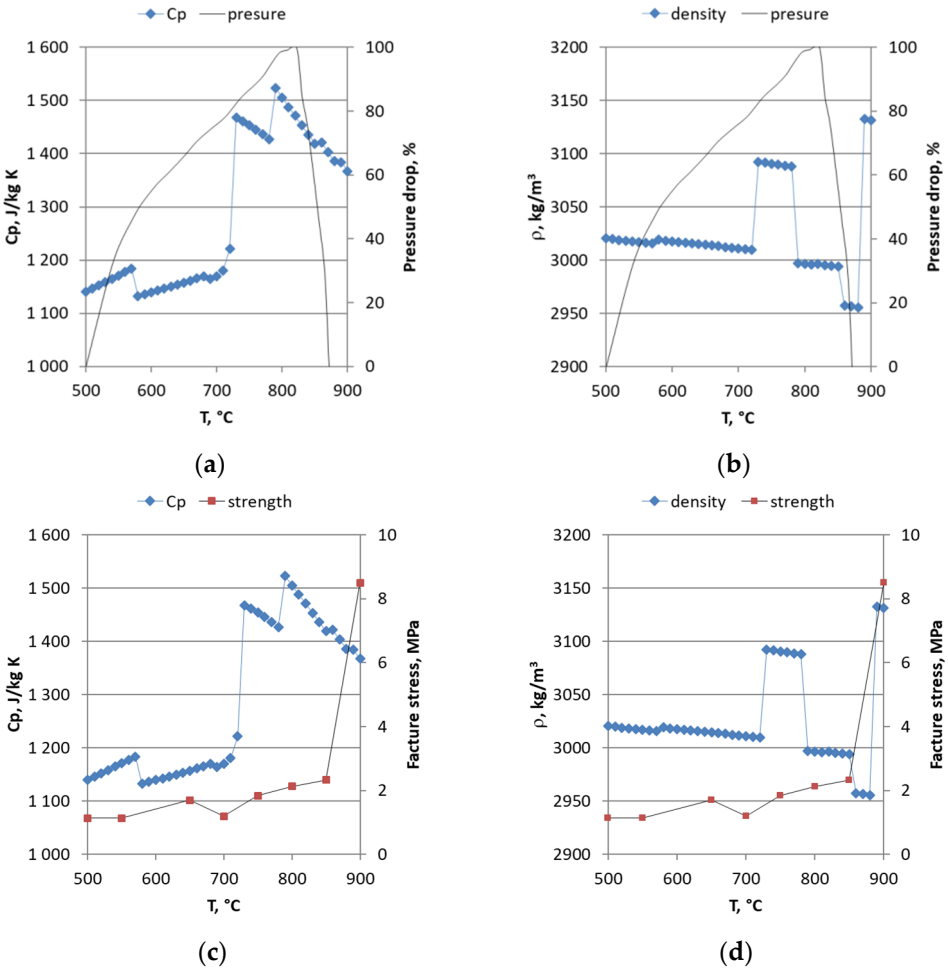

Figure 11. Lignite: (**a**) Specific heat (c_p) and pressure drop as a function of temperature; (**b**) density (ρ) and pressure drop as a function of temperature; (**c**) specific heat and fracture stress as a function of temperature; (**d**) density and fracture stress as a function of temperature.

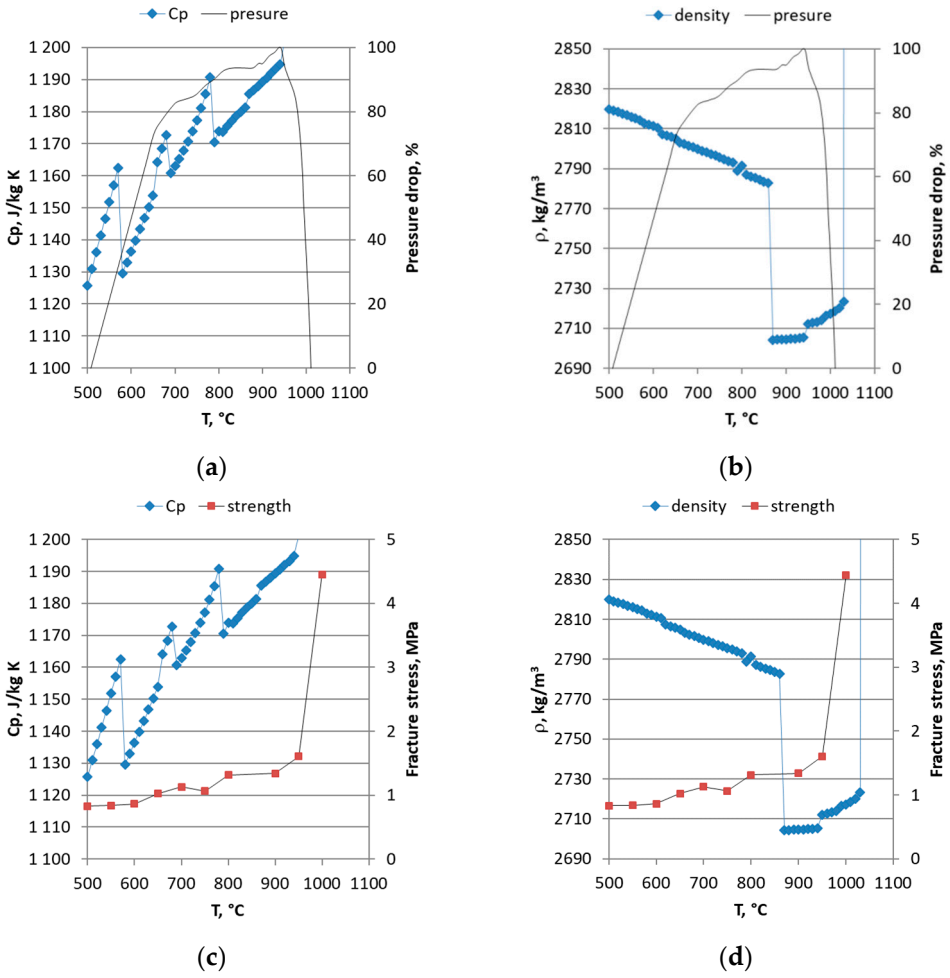

Figure 12. Bituminous coal: (**a**) Specific heat (c_p) and pressure drop as a function of temperature; (**b**) density (ρ) and pressure drop as a function of temperature; (**c**) specific heat and fracture stress as a function of temperature; (**d**) density and fracture stress as a function of temperature.

4. Conclusions

The presented research showed that nonstandard methods of ash sintering temperature testing, namely pressure and strength methods, are more reliable methods, reflecting the actual temperatures at which adverse changes in ash properties (sintering) begin to be observed, leading to such exploitation hazards as slagging or ashing. This is especially true for biomass, the chemical composition of which (high content of alkali metals) increases susceptibility to fouling and slagging.

Basic physicochemical tests and oxide analysis of the selected ash of the tested samples indicate very large differences in the ash properties. These differences are due not only to its smaller quantity in the case of biomass but also to its different oxide composition. Additionally, as the analyses showed, these ashes are characterized by an increase in the number of alkaline components, which are the main cause of the formation of hard-to-remove sinter.

Equilibrium simulations conducted using FactSage 8.0 software showed that there is a correlation between the parameters measured in the sintering temperature determination tests (pressure drop and the density of the fracture stress) and ash (without gas phase). Changes in the density of the samples clearly indicate that the ash sintering temperatures determined by the mechanical method and pressure drop test directly indicate the temperature at which the properties of the sample start to change. Changes in the properties of the ash indicate the start of its sintering process, which manifests itself as an increase in fracture stress (mechanical test) and pressure drop (pressure drop test).

Equilibrium simulations for the ash heat capacity c_p showed that the obtained characteristics $c_p = f(T)$ indicate the existence of rather pronounced points of discontinuity in these characteristics. These discontinuities are correlated with the ash sintering temperatures determined by the pressure drop test and the mechanical test.

The studies presented show that the mechanism of mineral transformation of fuels, especially biomass, is very complex. We are dealing with both chemical transformations (e.g., the formation of a slag phase) and physical transformations that involve not only phase transformations but also processes of changing the microstructure of the ash. This shows that non-standard methods, such as the mechanical test or the pressure drop test, have great potential to accurately determine the temperature at which the processes leading to ash and slag formation begin, especially because the process of transformation of the mineral substance of fuels, particularly biomass, is not fully recognized. In the article [47], the authors came to an interesting conclusion when studying the combustion of wood waste from the furniture industry. They found that on the basis of chemical analysis of deposits from domestic boilers, they can identify the fuel being burned.

Author Contributions: Conceptualization, K.K., W.M. and D.N.-W.; methodology, K.K., W.M. and D.N.-W.; validation, K.K., W.M. and D.N.-W.; formal analysis, K.K., W.M. and D.N.-W.; investigation, K.K., W.M. and D.N.-W.; resources, K.K., W.M. and D.N.-W.; data curation, K.K., W.M. and D.N.-W.; writing—original draft preparation, K.K., W.M. and D.N.-W.; writing—review and editing, K.K., W.M. and D.N.-W.; supervision, D.N.-W. All authors have read and agreed to the published version of the manuscript.

Funding: This research received no external funding.

Data Availability Statement: Not applicable.

Conflicts of Interest: The authors declare no conflict of interest.

References

1. Regulation (EU) 2021/1119 of the European Parliament and of the Council of 30 June 2021 Establishing the Framework for Achieving Climate Neutrality and Amending Regulations (EC) No 401/2009 and (EU) 2018/1999 ('European Climate Law'). Available online: http://data.europa.eu/eli/reg/2021/1119/oj (accessed on 25 November 2022).
2. Vassilev, S.V.; Baxter, D.; Vassileva, C.G. An overview of the behavior of biomass during combustion: Part II. Ash fusion and ash formation mechanisms of biomass types. *Fuel* **2014**, *117*, 152–183. [CrossRef]
3. Tchapda, A.H.; Pisupati, S.V. A Review of Thermal Co-Conversion of Coal and Biomass/Waste. *Energies* **2014**, *7*, 1098–1148. [CrossRef]
4. Nunes, L.; Matias, J.; Catalão, J. Biomass combustion systems: A review on the physical and chemical properties of the ashes. *Renew. Sustain. Energy Rev.* **2016**, *53*, 235–242. [CrossRef]
5. Niu, Y.Q.; Tan, H.Z.; Hụi, S.E. Ash related issues during biomass combustion: Alkali-induced slagging, silicate melt-induced slagging (ash fusion), agglomeration, corrosion, ash utilization and related countermeasures. *Prog. Energ. Combust.* **2016**, *52*, 1–61. [CrossRef]
6. Pophali, A.; Emami, B.; Bussmann, M.; Tran, H. Studies on sootblower jet dynamics and ash deposit removal in industrial boilers. *Fuel Process. Technol.* **2013**, *105*, 69–76. [CrossRef]
7. Kotelnikova, A.; Rogova, O.; Karpukhina, E.; Solopov, A.; Levin, I.; Levkina, V.; Proskurnin, M.; Volkov, D. Assessment of the structure, composition, and agrochemical properties of fly ash and ash-and-slug waste from coal-fired power plants for their possible use as soil ameliorants. *J. Clean. Prod.* **2021**, *333*, 130088. [CrossRef]
8. Sun, G.; Zhang, J.; Hao, B.; Li, X.; Yan, M.; Liu, K. Feasible synthesis of coal fly ash based porous composites with multiscale pore structure and its application in Congo red adsorption. *Chemosphere* **2022**, *298*, 134136. [CrossRef]
9. Zhou, H.; Luo, J.; Wang, Z.; Ji, M.; Zhang, M. Effect of walnut shell ash on pore structure characteristics during Zhundong coal sintering. *Fuel Process. Technol.* **2021**, *221*, 106923. [CrossRef]
10. Romdhane, L.; Ebinezer, L.B.; Panozzo, A.; Barion, G.; Cortivo, C.D.; Radhouane, L.; Vamerali, T. Effects of Soil Amendment With Wood Ash on Transpiration, Growth, and Metal Uptake in Two Contrasting Maize (*Zea mays* L.) Hybrids to Drought Tolerance. *Front. Plant Sci.* **2021**, *12*, 905. [CrossRef]
11. Hariana; Prabowo; Hilmawan, E.; Kuswa, F.M.; Darmawan, A.; Aziz, M. A comprehensive evaluation of cofiring biomass with coal and slagging-fouling tendency in pulverized coal-fired boilers. *Ain Shams Eng. J.* **2022**, 102001. [CrossRef]
12. Al-Otoom, A.Y.; Elliott, L.K.; Wall, T.F.; Moghtaderi, B. Measurement of the Sintering Kinetics of Coal Ash. *Energy Fuels* **2000**, *14*, 994–1001. [CrossRef]

13. Jing, N.; Wang, Q.; Luo, Z.; Cen, K. Effect of different reaction atmospheres on the sintering temperature of Jincheng coal ash under pressurized conditions. *Fuel* **2011**, *90*, 2645–2651. [CrossRef]
14. Shi, W.; Bai, J.; Kong, L.; Li, H.; Bai, Z.; Vassilev, S.V.; Li, W. An overview of the coal ash transition process from solid to slag. *Fuel* **2020**, *287*, 119537. [CrossRef]
15. Lim, J.; Kim, J. Optimizing ash deposit removal system to maximize biomass recycling as renewable energy for CO_2 reduction. *Renew. Energy* **2022**, *190*, 1006–1017. [CrossRef]
16. Raask, E. *Mineral Impurities in Coal Combustion: Behavior, Problems and Remedial Measures*; Hemisphere Publishing Corporation: Washington, DC, USA, 1985; Chapter 10; pp. 137–160.
17. Luan, C.; You, C.; Zhang, D. Composition and sintering characteristics of ashes from co–firing of coal and biomass in a la-boratory-scale drop tube furnace. *Energy* **2014**, *69*, 562–570. [CrossRef]
18. Jagodzińska, K.; Gądek, W.; Pronobis, M.; Kalisz, S. Investigation of ash deposition in PF boiler during combustion of torrefied biomass. In Proceedings of the IOP Conference Series: Earth and Environmental Science, Krakow, Poland, 14–17 November 2017; Volume 214, p. 012080.
19. Magdziarz, A.; Wilk, M.; Gajek, M.; Nowak-Woźny, D.; Kopia, A.; Kalemba-Rec, I.; Koziński, J. Properties of ash genarated during sewage sludge combustion: A multifaceded analysis. *Energy* **2016**, *113*, 85–94. [CrossRef]
20. Pronobis, M. Evaluation of the influence of biomass co-combustion on boiler furnace slagging by means of fusibility correlations. *Biomass-Bioenergy* **2005**, *28*, 375–383. [CrossRef]
21. Pronobis, M. The influence of biomass co-combustion on boiler fouling and efficiency. *Fuel* **2006**, *85*, 474–480. [CrossRef]
22. Vassilev, S.V.; Kitano, K.; Takeda, S.; Tsurue, T. Influence of mineral and chemical composition of coal ashes on their fusibility. *Fuel Process. Technol.* **1995**, *45*, 27–51. [CrossRef]
23. Polish Standard PN-ISO 540:2001 Solid Fuels—Determination of Ash Fusibility at High Temperature Using the Pipe Method. Available online: https://sklep.pkn.pl/pn-iso-540-2001p.html (accessed on 19 February 2021).
24. Du, S.; Yang, H.; Qian, K.; Wang, X.; Chen, H. Fusion and transformation properties of the inorganic components in biomass ash. *Fuel* **2014**, *117*, 1281–1287. [CrossRef]
25. Li, Q.; Zhang, Y.; Meng, A.; Li, L.; Li, G. Study on ash fusion temperature using original and simulated biomass ashes. *Fuel Process. Technol.* **2013**, *107*, 107–112. [CrossRef]
26. Król, K.; Nowak-Woźny, D. Application of the Mechanical and Pressure Drop Tests to Determine the Sintering Temperature of Coal and Biomass Ash. *Energies* **2021**, *14*, 1126. [CrossRef]
27. Al-Otoom, A.Y.; Bryant, G.W.; Elliott, L.K.; Skrifvars, B.J.; Hupa, M.; Wall, T.F. Experimental Options for Determining theTemperature for the Onset of Sintering of Coal Ash. *Energy Fuels* **2000**, *14*, 227–233. [CrossRef]
28. Jung, B.; Schobert, H.H. Viscous sintering of coal ashes. 2. Sintering behavior at short residence times in a drop tube furnace. *Energy Fuels* **1992**, *6*, 59–68. [CrossRef]
29. Vassilev, S.V.; Baxter, D.; Vassileva, C.G. An overview of the behavior of biomass during combustion: Part I. Phase-mineral transformations of organic and inorganic matter. *Fuel* **2013**, *112*, 393–449. [CrossRef]
30. Kleinhans, U.; Wieland, C.; Frandsen, F.J.; Spliethoff, H. Ash formation and deposition in coal and biomass fired combustion systems: Progress and challenges in the field of ash particle sticking and rebound behavior. *Prog. Energy Combust. Sci.* **2018**, *68*, 65–168. [CrossRef]
31. Sefidari, H.; Lindblom, B.; Wiinikka, H.; Nordin, L.-O.; Mouzon, J.; Bhuiyan, I.U.; Öhman, M. The effect of disintegrated iron-ore pellet dust on deposit formation in a pilot-scale pulverized coal combustion furnace. Part I: Characterization of process gas particles and deposits. *Fuel Process. Technol.* **2018**, *177*, 283–298. [CrossRef]
32. Sefidari, H.; Lindblom, B.; Wiinikka, H.; Nordin, L.-O.; Lennartsson, A.; Mouzon, J.; Bhuiyan, I.U.; Öhman, M. The effect of disintegrated iron-ore pellet dust on deposit formation in a pilot-scale pulverized coal combustion furnace. Part II: Thermochemical equilibrium calculations and viscosity estimations. *Fuel Process. Technol.* **2018**, *180*, 189–206. [CrossRef]
33. Sefidari, H.; Wiinikka, H.; Lindblom, B.; Nordin, L.; Wu, G.; Yazhenskikh, E.; Müller, M.; Ma, C.; Öhman, M. Comparison of high-rank coals with respect to slagging/deposition tendency at the transfer-chute of iron-ore pelletizing grate-kiln plants: A pilot-scale experimental study accompanied by thermochemical equilibrium modeling and viscosity estimations. *Fuel Process. Technol.* **2019**, *193*, 244–262. [CrossRef]
34. Sefidari, H. Mechanisms of Deposit Formation in the Grate-Kiln Process. Ph.D. Thesis, Luleå Tekniska Universitet, Luleå, Sweden, 2018. Available online: https://scholar.google.com/scholar_lookup?title=Mechanisms%20of%20Deposit%20Formation%20in%20the%20Grate-Kiln%20Process&publication_year=2018&author=H.%20Sefidari (accessed on 25 November 2022).
35. Atallah, E.; Defoort, F.; Pisch, A.; Dupont, C. Thermodynamic equilibrium approach to predict the inorganic interactions of ash from biomass and their mixtures: A critical assessment. *Fuel Process. Technol.* **2022**, *235*, 107369. [CrossRef]
36. Daley, P.; Reinmöller, M.; Williams, O.; Pang, C.H.; Lester, E. The influence of mineral addition on the Optimised Advanced Ash Fusion Test (OAAFT) and its thermochemical modelling and prediction. *J. Energy Inst.* **2022**, *105*, 121–132. [CrossRef]
37. Magdziarz, A.; Gajek, M.; Nowak-Woźny, D.; Wilk, M. Mineral phase transformation of biomass ashes–Experimental and thermochemical calculations. *Renew. Energy* **2018**, *128*, 446–459. [CrossRef]
38. Kaniowski, W.; Taler, J.; Wang, X.; Kalemba-Rec, I.; Gajek, M.; Mlonka-Mędrala, A.; Nowak-Woźny, D.; Magdziarz, A. Investigation of biomass, RDF and coal ash-related problems: Impact on metallic heat exchanger surfaces of boilers. *Fuel* **2022**, *326*, 125122. [CrossRef]

39. Nowak-Woźny, D.; Ferens, W.; Wach, J. Using dissipation factor method in testing the ash sintering process of cereal pellet and coal fuels. *Energy* **2022**, *250*, 123718. [CrossRef]
40. CEN/TS 14775:2004 Solid Biofuels-Method for the Determination of Ash Content. Available online: https://standards.iteh.ai/catalog/standards/sist/7a423bc5-65a2-40ae-90f7-319c45968a59/sist-ts-cen-ts-14775-2004 (accessed on 25 November 2022).
41. *Polish Standard PN-G-04502:2014-11*; Hard and Brown Coals—Sampling and Preparation of Samples for the Laboratory Tests—Primary Methods. ISO: London, UK, 2014.
42. *Polish Standard PN-EN ISO 18134-1:2015-11*; Solid Biofuels—Determination of Moisture Content—Oven Dry Meth-od—Part 1: Total Moisture—Reference Method. ISO: London, UK, 2015.
43. *Polish Standard PN-EN ISO 18123:2016-01*; Solid Biofuels—Determination of the Content of Volatile Matter. ISO: London, UK, 2015.
44. *Polish Standard PN-EN ISO 18122:2016-01*; Solid Biofuels—Determination of Ash Content. ISO: London, UK, 2015.
45. *Polish Standard PN-ISO 1928:2020-05*; Solid Mineral Fuels—Determination of Gross Calorific Value by the Bomb Calo-rimetric Method and Calculation of Net Calorific Value. ISO: London, UK, 2020.
46. Sato, R.; Kadoma, T.; Fujimoto, Y.; Ogata, N.; Yabuuchi, K.; Ninomiya, Y.; Horio, M. Clinker Formation Behavior in a Co-current Up-flowing Moving Bed Gasifier Fueled with Japanese Cedar Pellets. *J. Jpn. Inst. Energy* **2021**, *100*, 236–244. [CrossRef]
47. Růžičková, J.; Raclavská, H.; Juchelková, D.; Šafář, M.; Kucbel, M.; Švédová, B.; Slamová, K.; Grobelak, A. The use of polymer compounds in the deposits from the combustion of briquettes in domestic heating as an identifier of fuel quality. *Environ. Sci. Pollut. Res.* **2021**, 1–19. [CrossRef]